MATERIALS PROCESSING FUNDAMENTALS 2018

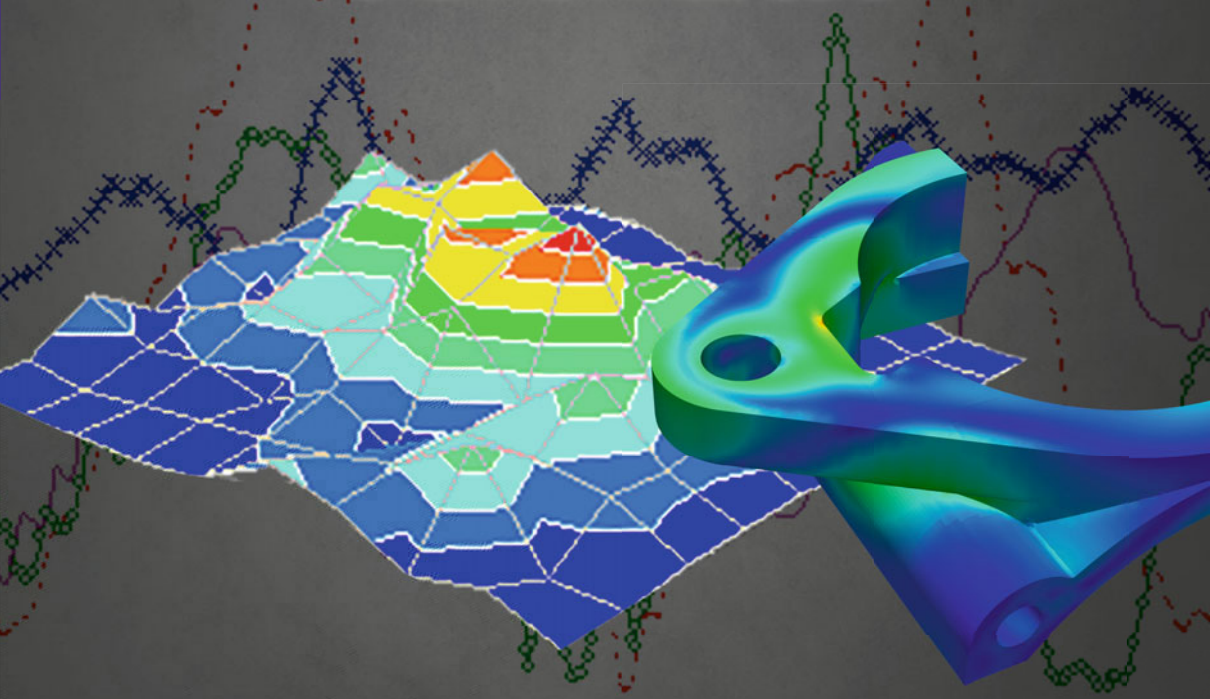

Edited by
Guillaume Lambotte • Jonghyun Lee
Antoine Allanore • Samuel Wagstaff

TMS

Springer

The Minerals, Metals & Materials Series

Guillaume Lambotte · Jonghyun Lee
Antoine Allanore · Samuel Wagstaff
Editors

Materials Processing Fundamentals 2018

TMS

Springer

Editors
Guillaume Lambotte
Boston Electrometallurgical Corporation
Woburn, MA
USA

Antoine Allanore
Massachusetts Institute of Technology
Cambridge, MA
USA

Jonghyun Lee
Iowa State University
Ames, IA
USA

Samuel Wagstaff
Novelis
Sierre
Switzerland

ISSN 2367-1181 ISSN 2367-1696 (electronic)
The Minerals, Metals & Materials Series
ISBN 978-3-319-72130-9 ISBN 978-3-319-72131-6 (eBook)
https://doi.org/10.1007/978-3-319-72131-6

Library of Congress Control Number: 2017960289

Printed on acid-free paper

This Springer imprint is published by Springer Nature
The registered company is Springer International Publishing AG
The registered company address is: Gewerbestrasse 11, 6330 Cham, Switzerland

Preface

The symposium Materials Processing Fundamentals is hosted at the annual meeting of The Minerals, Metals & Materials Society (TMS) as the flagship symposium of the Process Technology and Modeling Committee. It is a unique opportunity for interdisciplinary presentations and discussions about, among others, processing, sensing, modeling, multi-physics, computational fluid dynamics, and thermodynamics.

The materials covered include ferrous and nonferrous elements, and the processes range from mining unit operations to joining and surface finishing of materials. Acknowledging that modern processes involve multi-physics, the symposium and its proceedings allow the reader to learn the methods and outcome of other fields modeling practices, often enabling the development of practical solutions to common problems. Modeling of basic thermodynamic and physical properties play a key role, along with computer fluid dynamics and multiphase transport and interface modeling.

Contributions to the proceedings include applications such as steel processing, modeling of steel and nonferrous alloys treatments for properties control, multi-physics, and computational fluid dynamics modeling for molten metal processes and properties measurement. Extractive, recovery, and recycling process modeling are also presented, completing a broad view of the field and practices of modeling in materials processing.

The engagement of TMS and committee members to chair sessions, review manuscript, and help TMS present current practices, makes this symposium and its proceedings possible. The editor and its coeditors acknowledge the invaluable support and contribution of these volunteers as well as TMS staff members, in particular, Patricia Warren, Trudi Dunlap, Carol Matty, and Matt Baker.

Guillaume Lambotte
Jonghyun Lee
Antoine Allanore
Samuel Wagstaff

Contents

Part I Steelmaking—Processing

The Effect of a Sulfur Addition on the Formation and Behavior of CaS Inclusions During a Secondary Refining Process Without Using a Ca-Treatment 3
Takanori Yoshioka, Yuta Shimamura, Andrey Karasev, Yasuhide Ohba and Pär Göran Jönsson

Desulfurization of Copper-Iron Reduced from Copper Slag 15
Bao-jing Zhang, Ting-an Zhang, Li-ping Niu, Zhi-he Dou, Zhi-qiang Li and Dong-liang Zhang

Part II Steelmaking—Properties

Effects of Aging Treatment on the Microstructure and Mechanical Properties of a Nanoprecipitates-Strengthened Ferritic Steel 27
Y. Zhao, Y. Cui, H. Guo, S. S. Xu, X. H. Wei and Z. W. Zhang

Part III Multiphysics—Process Modeling and Sensing

Convection-Diffusion Model of Lithium-Bismuth Liquid Metal Batteries 41
Rakan F. Ashour and Douglas H. Kelley

Study on Emulsion Phenomena and Field Flow Pattern in Side-Blown Copper Smelting Process 53
Xiao-long Li, Ting-an Zhang, Yan Liu and Dong-xing Wang

Study on Minimum Starting Energy of Self-stirring Reactor Driven By Pressure Energy 65
Zimu Zhang, Qiuyue Zhao, Maoyuan Li, Xuhuan Guo, Dianhua Zhang and Ting-an Zhang

Part IV Alloy Processing and Properties Modeling

Yield Strength Prediction in 3D During Local Heat Treatment of Structural A356 Alloy Components in Combination with Thermal-Stress Analysis 77
Tobias Holzmann, Andreas Ludwig and Peter Raninger

Thermodynamic Properties of Magnetic Semiconductors $Ag_2FeSn_3S_8$ and Ag_2FeSnS_4 Determined by the EMF Method 87
Mykola Moroz, Fiseha Tesfaye, Pavlo Demchenko, Myroslava Prokhorenko, Daniel Lindberg, Oleksandr Reshetnyak and Leena Hupa

Effects of Heat Treatment on the Electrochemical Performance of Al Based Anode Materials for Air-Battery 99
Xingyu Gao, Jilai Xue, Xuan Liu and Gaojie Shi

Part V Extractive and Recovery Processing

A Current Efficiency Prediction Model Based on Electrode Kinetics for Iron and Copper During Copper Electrowinning 111
Zongliang Zhang, Joshua Werner and Michael Free

The K_2SO_4–$CaSO_4$ System and Its Role in Fouling and Slagging During High-Temperature Processes 133
Fiseha Tesfaye, Daniel Lindberg and Leena Hupa

Waste Lithium-Ion Battery Recycling in JX Nippon Mining & Metals Corporation 143
Yasufumi Haga, Katsumi Saito and Kazuhiro Hatano

Recovery of Platinum Group Metals Out of Automotive Catalytic Converters Scrap: A Review on Australian Trends and Challenges 149
Maryam Ghodrat, Pezhman Sharafi and Bijan Samali

Leaching Recovery of Silver from Used Radiographic Films 163
A. A. Adeleke, A. N. Adebayo, B. O. Ibitoye and K. E. Oluwabunmi

The Study of Copper Leaching from Conichalcite and Chalcopyrite Using Alternative Lixiviants 171
Junmo Ahn, Isabel F. Barton, Doyun Shin and Jaeheon Lee

Effect of Chloride Ions on the Copper Extraction Using LIX 984N and Acorga M5910 181
M. C. Ruiz, J. Risso, R. Sanchez and R. Padilla

$CaCl_2$–O_2 Roasting of Stibnite and a Complex Copper Concentrate at 500–650 °C 189
R. Padilla, G. Brito and M. C. Ruiz

Research on Sulfur Conversion Behavior in Oxygen Pressure Acid Leaching Process of High Indium Sphalerite 199
Yan Liu, Yang-yang Fan, Jun-fu Qi, Lei Tian and Ting-an Zhang

Part VI Poster Session

Hybrid Modeling for Endpoint Carbon Content Prediction in EAF Steelmaking 211
Guang-sheng Wei, Rong Zhu, Lingzhi Yang and Tianping Tang

DEM Simulation of Dispersion of Cohesive Particles by Spontaneous Inter-particle Percolation in a 3D Random Packed Bed 225
Heng Zhou, Sheng-li Wu, Ming-yin Kou, Shun Yao, Bing-jie Wen, Kai Gu and Feng Chang

Author Index 237

Subject Index 239

About the Editors

Guillaume Lambotte is a Senior Research and Development Scientist at Boston Electrometallurgical Corporation, a Massachusetts Institute of Technology (MIT) spin-off start-up focusing on the development of an environmentally friendly and energetically efficient primary metal extraction process. Dr. Lambotte primarily focuses on computational thermodynamic modeling, electrochemistry, and high-temperature equilibrium. Prior to joining BEMC, he conducted research as a postdoctoral associate at the University of Massachusetts (UMass) Amherst and MIT. Before his graduate studies, Dr. Lambotte worked as a Production Assistant Manager at Alcan Extruded Products (Crailsheim, Germany).

Dr. Lambotte obtained his bachelor degree from the European Engineer School for Materials Science (Nancy, France). He received his M.Sc. and Ph.D. in metallurgical engineering from Ecole Polytechnique of Montreal (Montreal, Canada).

Dr. Lambotte is currently serving as the chair of the TMS Process Technology and Modeling Committee and was the recipient of the 2015 TMS EPD Young Leaders Professional Development Award. In 2015, Dr. Lambotte was one of the TMS representatives at the Emerging Leaders Alliance Conference.

Jonghyun Lee is an Assistant Professor in the Department of Mechanical Engineering at Iowa State University. He has been conducting multiple industry- and government-funded projects in the field of materials processing as PI and Co-I.

Dr. Lee was the recipient of the Young Leaders Professional Development Award in 2013 from The Minerals, Metals & Materials Society, where he has been serving as a co-organizer and coeditor of the Materials Processing Fundamentals Symposium since 2014 and as a vice-chair of the Process Modeling and Technology Committee since 2017.

Prior to joining his current institution, Dr. Lee was a Research Assistant Professor at the University of Massachusetts Amherst. He also had nearly 5 years of industry experience and worked as a postdoctoral associate at Tufts University, Medford, Massachusetts. He earned his M.S. and Ph.D. in mechanical engineering from the University of Massachusetts Amherst and his B.S. in the same discipline from Inha University in Incheon, South Korea.

Antoine Allanore is an Associate Professor of Metallurgy in the Department of Materials Science and Engineering at MIT. He received his higher education in Nancy (France), where he earned a chemical process engineer diploma from Ecole Nationale Supérieure des Industries Chimiques and a M.Sc. and a Ph.D. from Lorraine University.

Dr. Allanore joined MIT in 2012 as a faculty member, leading a research group that develops sustainable materials extraction and manufacturing processes. He has developed numerous alternative approaches for metals and minerals extraction and processing. With an emphasis on electrochemical methods for both analytical and processing purposes, his group combines experimental and modeling approaches to promptly investigate the ultimate state of condensed matter, the molten state. He teaches thermodynamics and sustainable chemical metallurgy at both the undergraduate and graduate level.

He received the Vittorio de Nora Award from TMS in 2012, and the TMS Early Career Faculty Fellow Award in 2015.

Samuel Wagstaff has been working in the aluminum industry since age 14 with Novelis in Spokane, Washington. He received his B.S. from Cornell University in Mechanical and Aerospace Engineering in 2013. He continued his education at the Massachusetts Institute of Technology in the Department of Materials Science and Engineering.

His Ph.D. on the minimization of macrosegregation through jet erosion of a continuously cast ingot uses a turbulent jet to reduce the uneven distribution in aluminum alloy ingots by over 70 %. Dr. Wagstaff finished his masters and doctorate at MIT in September 2016 after just 3 years. He has published more than a dozen articles on DC casting and macrosegregation, and holds 12 patents. He now works for Novelis in Sierre, Switzerland as an Automotive Development and Process Engineer.

Part I
Steelmaking—Processing

The Effect of a Sulfur Addition on the Formation and Behavior of CaS Inclusions During a Secondary Refining Process Without Using a Ca-Treatment

Takanori Yoshioka, Yuta Shimamura, Andrey Karasev, Yasuhide Ohba and Pär Göran Jönsson

Abstract This study aimed to elucidate the effect of a sulfur addition on the formation and behavior of CaS inclusions in steel melts during a secondary refining process without a Ca-treatment. Samples were taken during production for two different steel grades, namely a low-S steel (S = 0.005%) and a high-S steel (S = 0.055%). Thereafter, the inclusion characteristics were determined using an SEM combined with an EDS. The results show that the CaO content in the inclusions decreased and the CaS content increased after a sulfur addition during an RH process for the high-S steel. Furthermore, CaS-covered inclusions were frequently detected in the high-S steel samples after the S addition. Thermodynamic calculations were also performed to compare the CaS formation behavior in the two steels. The results showed that a CaS phase can thermodynamically be formed in the high-S steel melt even without a Ca-treatment. Also, it was indicated that a CaS phase can be formed in two ways, namely a reaction between Ca and S and a reaction between CaO in inclusions and S. From the viewpoint of interfacial features, inclusions covered by a CaS phase are thought to possess low contact angles to steel melts. Therefore, CaS-covered inclusions tend to remain in a steel melt. According to the results of this study, CaS inclusions can be formed and deteriorate the castability of high-S containing steels even without a Ca-treatment.

Keywords CaS inclusion · High-S · Ca-treatment · Castability
Thermodynamics · Contact angle

T. Yoshioka (✉) · A. Karasev · P. G. Jönsson
Department of Materials Science and Engineering,
KTH Royal Institute of Technology, Stockholm, Sweden
e-mail: tyoshioka@himeji.sanyo-steel.co.jp

T. Yoshioka · Y. Shimamura · Y. Ohba
Process Research Group, Basic Research Office,
Research & Development Center, Sanyo Special Steel Co., Ltd., Himeji, Japan

G. Lambotte et al. (eds.), *Materials Processing Fundamentals 2018*,
The Minerals, Metals & Materials Series,
https://doi.org/10.1007/978-3-319-72131-6_1

Introduction

Inclusions can be detrimental to a stable casting when they exist in a solid phase at steelmaking temperatures [1]. Generally, solid oxide inclusions have high interfacial energies to steel melts [2]. Therefore, they tend to accumulate on a nozzle wall which can cause a nozzle clogging [1, 3, 4]. In addition to solid oxide inclusions, CaS inclusions are also recognized as being harmful for a high castability since they also exist as a solid phase at steelmaking temperatures [1, 3, 4]. Therefore, the activities of steel components such as Ca, S, and Al should be controlled carefully when a Ca-treatment is performed [1, 3, 4]. However, a high-S content in a steel product is sometimes required to possess a high machinability. This high-S content leads to a high activity of S, which can react with Ca or a CaO phase in a steel melt and generate a CaS phase. However, there are still few discussions on the formation and behavior of CaS inclusions without using a Ca-treatment. From this standpoint, this study aimed to clarify the formation and behavior of CaS inclusions in steel melts without using a Ca-treatment. In practice, steel samples were taken from the ladle during a secondary refining process. Thereafter, the CaS formation and its behavior in a steel melt were discussed.

Experimental Procedures

The procedure of the melt shop is an EAF → LF → RH → CC line. Two steel grades were subject to this study, namely steel A (0.20%C–0.26%Si–0.83%Mn–0.005%S) and steel B (0.36%C–0.76%Si–1.33%Mn–0.055%S) to investigate the effect of the S content on the formation behavior of CaS inclusions in a steel melt. These two steels are manufactured with high basicity slags, which had a composition saturated with both CaO and MgO. During the production of steel B, its high S content was adjusted during an RH treatment since slag/metal reactions are not active during the process. Steel samples were taken at the end of the LF refining (45 min) and the RH treatment (25 min). These samples were named “LF end” and “RH end”, respectively. The compositions of inclusions on the polished cross section of each steel sample were analyzed using an SEM/EDS inclusion analyzer. The scanned area was 100 mm^2. To calculate the content of CaO in the inclusions, the measured small amount of Mn was allotted to an MnS phase and the remaining S was considered to be bound as a CaS phase. After this procedure, the rest of the Ca content was allotted to a CaO phase [5, 6]. The methods for quantitative analyses of steel compositions were the same as presented in the previous work [6]. To discuss variations of inclusion compositions, the Ca content in each steel sample was calculated based on the information of the average inclusion composition and insoluble oxygen content (T.O - O_{calc}) at each sampling time. A detailed explanation of this calculation is described in previous papers [7, 8].

Results

Variations of Compositions in the Steel Melts

The variations of the steel compositions during the processes are shown in Fig. 1. The sulfur contents in both steels were reduced below 0.005 mass% at the end of the LF refining process. Thereafter, FeS was added into the steel melts to enable their products to possess designed steel properties. The increase in Al in steel B is a result of an Al addition which aimed to compensate Al consumption during an RH treatment [6, 9]. The Ca contents in the steel melts were around 5 ppm at the end of the LF refining and thereafter decreased below 1 ppm after the following RH treatment. This decrease can be due to vaporization of Ca into a gas phase [10], or reactions between Ca and other elements during the RH treatment.

Variations of Inclusion Compositions

The variations of the inclusion compositions in each steel are shown in Fig. 2. The compositions of inclusions are plotted in two diagrams: a CaO–MgO–Al_2O_3 ternary diagram and a CaO–CaS–Al_2O_3 ternary diagram. The open circles in these figures represent the number-averaged composition at each step. At the end of the LF refining, the inclusion compositions were placed on the tie-line connecting the areas of $MgO \cdot Al_2O_3$ and CaO–Al_2O_{3liq} (CaO–Al_2O_{3liq}: mass%CaO = 36–58 at 1873 K [11]) in both steels. This result is consistent with the result which has been reported by Yoshioka et al. [6]. The results also showed that some of the inclusions already contained various amounts of CaS at this stage of the LF treatment.

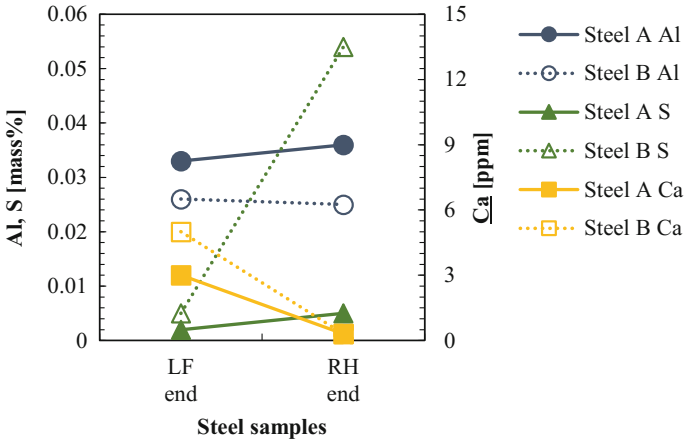

Fig. 1 Variations of the steel compositions in steel A and steel B during the LF-RH process

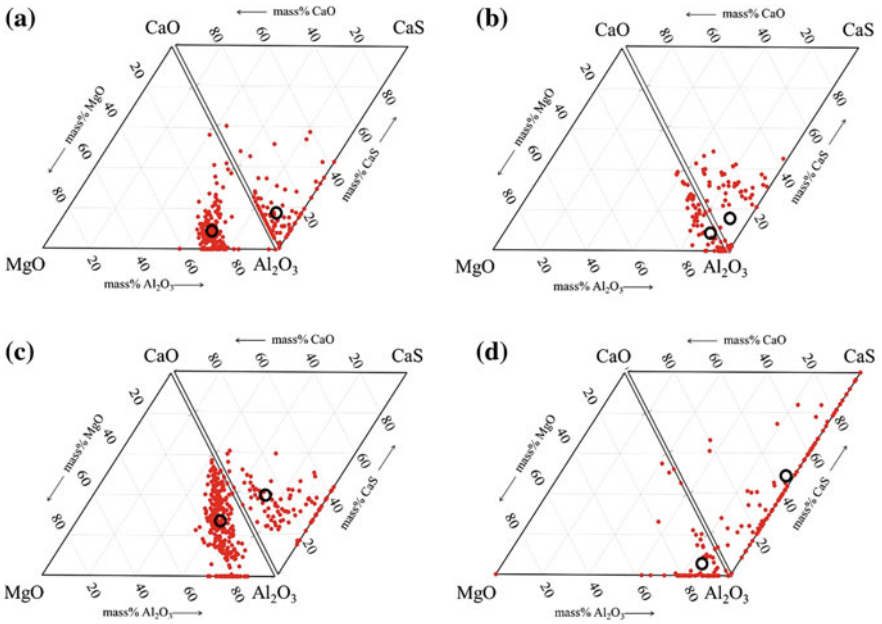

Fig. 2 Inclusion compositions in each sample: **a** LF end of steel A, **b** RH end of steel A, **c** LF end of steel B, **d** RH end of steel B

The difference in the CaS contents in inclusions between the two grades might be due to the difference in the Ca and S contents during the LF refining process. After the RH treatment, the inclusions in steel A mainly consisted of three phases, namely Al_2O_3, CaO–Al_2O_{3liq}, and CaS. On the other hand, the inclusions mainly consisted of two phases, Al_2O_3 and CaS in steel B. In addition to this difference, the CaS contents in the inclusions in steel B were much higher (steel A: 6.9 mass%, steel B: 42.9 mass% in the average composition normalized in the CaO–MgO–Al_2O_3–CaS quarterly system) than those in steel A. Overall, the inclusion compositions were not significantly different between the two steels at the end of the LF refining. However, at the end of the RH treatment, the inclusion compositions were quite different between the two steels with respect to the CaO and CaS contents.

Figure 3 shows the results of SEM observations of the typical inclusion found in each sample. In the samples taken at the end of the LF treatment in both steel grades, the inclusions consisted of two phases, namely a CaO–Al_2O_3 phase and an MgO · Al_2O_3 phase (Fig. 3a, c). At the end of the RH treatment, Al_2O_3 inclusions were observed in the sample of steel A (Fig. 3b). In the sample of steel B, inclusions surrounded by a CaS phase were frequently observed after the RH treatment (Fig. 3d). These observed results agree with the variations of the inclusion compositions shown in Fig. 2.

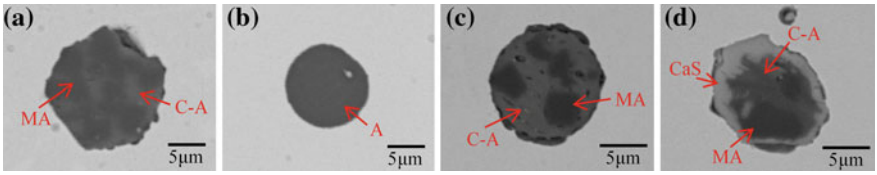

Fig. 3 SEM observations of a typical inclusion found at each stage of the ladle treatment: **a** LF end of steel A, **b** RH end of steel A, **c** LF end of steel B, **d** RH end of steel B

Discussion

Thermodynamic Consideration

As mentioned above, CaS inclusions were observed in the sample of steel B at the end of the RH treatment although no Ca-treatment was used. In the following section, the possible reasons for the CaS formation are discussed from a thermodynamic viewpoint.

CaS Formation by a Reaction Between Ca and S in a Steel Melt

One way to form a CaS phase is due to a reaction between Ca and S in a steel melt. This reaction is expressed in Eq. (1) [12].

$$\underline{\mathrm{Ca}} + \underline{\mathrm{S}} = \mathrm{CaS(s)} \quad \Delta G_1^0 = -530000 + 115.6T\,[\mathrm{J/mol}] \tag{1}$$

A CaS stability diagram was calculated at 1873 and 1823 K, which represent the operation temperatures of the LF refining and the RH treatment, respectively. In this calculation, the interaction parameters shown in Table 1 were used [12–14]. The activities of Ca (a_{Ca}) and S (a_{S}) were calculated with the following Eqs. (2) and (3), where f_i is the activity coefficient of element i in a steel melt.

Table 1 Interaction parameters (e_i^j) of the main elements in the steel melt used in the present study*

j / i	C	Si	Mn	Al	Ca	O
Ca	−0.34	−0.096	−0.0156	−0.072	−0.002	−9000 [14]
Al	0.091	0.056	−0.004	0.043	−0.047	−6.6 [12]
O	−0.45	−0.131	−0.021	−3.9 [12]	−3600 [14]	−0.17
S	0.11	–	−0.026	0.041	−269 [12]	−0.27

*(All data without notation were taken from Ref. [13])

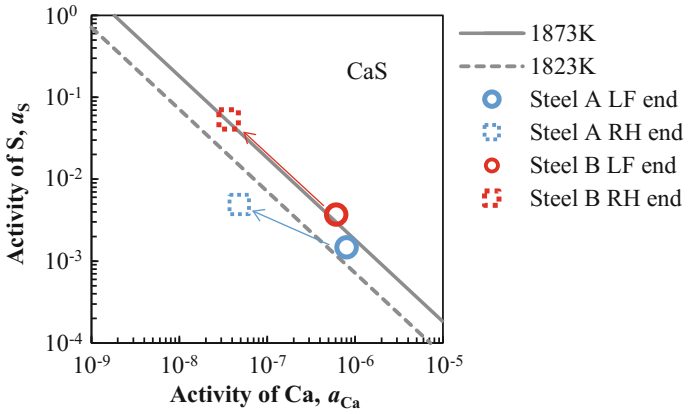

Fig. 4 Stability diagram of CaS formed by a reaction between Ca and S in steel melts

$$a_i = f_i \cdot [\text{mass\% i}] \tag{2}$$

$$logf_i = \sum e_i^j \cdot [\text{mass\% j}] \tag{3}$$

Moreover, the activity of the CaS phase was taken as unity due to its small solubility in CaO–Al_2O_3 phases [15]. Figure 4 shows the obtained relationships between the CaS stability and the activities of Ca and S in steel melts. The symbols in the figure correspond to the Ca and S activities at each sample.

According to this result, Ca and S cannot thermodynamically react to form a CaS phase at the end of the LF refining in any of the two studied steels. Furthermore, CaS cannot be formed in steel A during the RH treatment due to the low Ca and S activities. On the other hand, CaS can be formed in steel B due to the high S activity.

CaS Formation Due to a Reaction Between CaO in Inclusions and S in a Steel Melt

Another way to form a CaS phase in a steel melt is due to a reaction between CaO in inclusions and S. This reaction can be expressed as shown in Eq. (5), which was derived by combining Eqs. (1) and (4) [12].

$$\underline{\text{Ca}} + \underline{\text{O}} = \text{CaO(s)} \quad \Delta G_2^0 = -644000 + 148.1T\,[\text{J/mol}] \tag{4}$$

$$\text{CaO(s)} + \underline{\text{S}} + \frac{2}{3}\underline{\text{Al}} = \text{CaS(s)} + \frac{1}{3}\text{Al}_2\text{O}_3 \quad \Delta G_3^0 = -294500 + 98.8T\,[\text{J/mol}] \tag{5}$$

As can be seen in Eq. (5), the progress of this reaction also depends on the activities of CaO and Al_2O_3 in the inclusions. This reaction can easily occur when the CaO activity is high and the Al_2O_3 activity is low. Table 2 shows the activities of CaO and Al_2O_3 at each boundary of the CaO–Al_2O_3 system which was calculated using the thermodynamic software Factsage [6]. These activity data were substituted into Eq. (5) to identify the effect of the inclusion phases. Here, the activity of CaS was set as unity in this calculation.

Figure 5 shows the calculated relationships between the activities of Al and S to form a CaS phase by the reaction of Eq. (5). The plots in the figure correspond to the Al and S activities at each sample. As has been frequently reported, a CaO–Al_2O_{3liq} phase is the most stable oxide in an Al-killed steel melt [6, 16–18]. Based on the result shown in Fig. 5, the CaO–Al_2O_{3liq} phase can coexist with a CaS phase under a low S activity condition. In the current study, this condition prevails at the end of the LF treatment for both steels and at the end of the RH treatment for steel A. At the end of the RH treatment in steel B, the activity of S is greatly increased from 0.004 to 0.05 by the FeS addition. Therefore, the modified CaO–Al_2O_3 phases, such as CaO · Al_2O_3 and CaO–Al_2O_{3liq}, can react with S to form a CaS phase. This reaction contributes to both a decrease in the CaO contents and an increase in the CaS contents in inclusions in a steel melt, which were seen in Figs. 2c, d.

Table 2 Activities of CaO and Al_2O_3 in various boundaries of a CaO–Al_2O_3 system at 1873 K [6]

Boundary	a_{Al2O3}	a_{CaO}
Al_2O_3(s)/CaO·6Al_2O_3(s)	1.0	0.0049
CaO·6Al_2O_3(s)/CaO·2Al_2O_3(s)	0.88	0.010
CaO·2Al_2O_3(s)/CaO·Al_2O_3(s)	0.29	0.10
CaO·Al_2O_3(s)/CaO–Al_2O_3(l)	0.18	0.17
CaO–Al_2O_3(l)/CaO(s)	0.0089	0.99

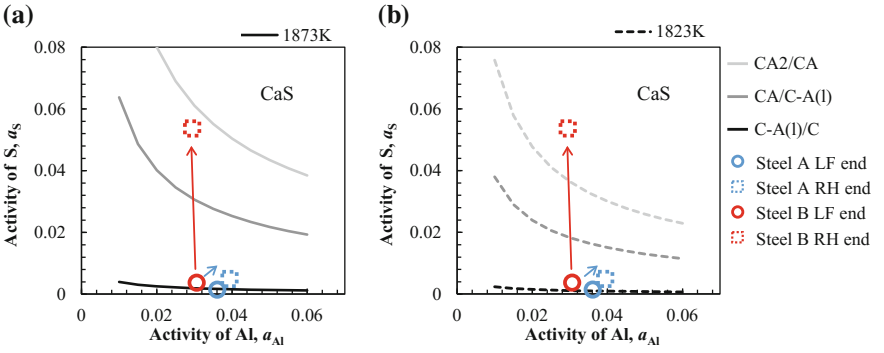

Fig. 5 Relationships between the activities of Al and S to form a CaS phase by a reaction between CaO in various CaO–Al_2O_3 phases and S in steel melts at **a** 1873 K and **b** 1823 K. (C: CaO, A: Al_2O_3)

Overall, the results in this study indicate that a CaS phase can be formed in a steel melt even when a Ca-treatment has not been used. The reactions for this CaS formation can progress in two manners, namely due to a reaction between Ca and S and due to a reaction between CaO in inclusions and S. These reactions are thought to progress at the inclusion/metal interface. This is the explanation to why the inclusions in the production of steel B were covered by a CaS phase after the FeS addition.

Behavior of CaS Inclusions in a Steel Melt

The removal tendency of an inclusion from a steel melt is greatly affected by an interfacial property, namely the contact angle between an inclusion and a steel melt [19–21]. Arai et al. have clearly elucidated the effect of contact angles on the removal behavior of particles in a liquid [19]. According to their work, the removal tendency steeply decreases when the contact angle between an inclusion and a steel becomes lower than 90°. Generally, solid oxides such as Al_2O_3, $CaO–Al_2O_3$ with low CaO contents, and $MgO \cdot Al_2O_3$ have large contact angles in contact to steel melts (>90°) [2]. This information means that solid oxides are easy to remove from a melt. On the other hand, liquid oxides, such as $CaO–Al_2O_{3liq}$, have small contact angles (50°–60° [2]), so they are difficult to remove from a steel melt. The contact angle of a CaS phase to a steel melt has been reported as 87° [22]. The S content, mentioned in ref. [22], in the steel melt is 0.01 mass%. Sulfur is well-known to be a surface active element, which can decrease the interfacial energies of slag/metal and inclusion/metal interfaces [23, 24]. By considering the sulfur content of high-S steels (around 0.05 mass% as shown in Fig. 1), the contact angles of a CaS phase to the steel melts are thought to be 87° or less. Therefore, it can be implied that CaS-covered inclusions, which were identified in Figs. 2d and 3d, are difficult to remove, and they tend to remain in a steel melt even after the completion of an RH treatment.

As mentioned above, liquid inclusions and CaS inclusions are difficult to remove from a steel melt. However, liquid inclusions rarely cause a nozzle clogging even if they remain in a steel melt after refining processes. On the other hand, CaS inclusions are well-known to deteriorate the castability since they exist as solid inclusions in a steel melt (melting point ≈ 2800 K) [1, 3, 4, 11]. Thus, CaS inclusions have quite undesirable characteristics such as a tendency to remain in a steel melt and a tendency to accumulate on a nozzle wall, which can causes a nozzle clogging. Table 3 summarizes the results of this discussion.

A deposition on a nozzle wall of a ladle after casting steel B was investigated using an SEM in combination with an EDS. The result is shown in Fig. 6. As seen, sulfides were frequently detected in the deposition. Thus, CaS inclusions can cause a clogging in production of high-S steels even for cases where a Ca-treatment has not been used.

Table 3 Dominant inclusion types and their behavior in low-S steel melts and in high-S steel melts

Inclusion type	Removal from a melt	Clogging	In low-S steels without a Ca-treatment	In high-S steels without a Ca-treatment
Solid oxide*	Preferable (easy)	Unpreferable (can cause)	Dominant (Clogging cannot occur if solid inclusions are properly removed)	–
Liquid oxide*	Unpreferable (difficult)	Preferable (cannot cause)		
CaS inclusion	Unpreferable (difficult)	Unpreferable (can cause)	–	dominant (CaS inclusions tend to remain in steel melts and cause cloggings)

*At a steelmaking temperature

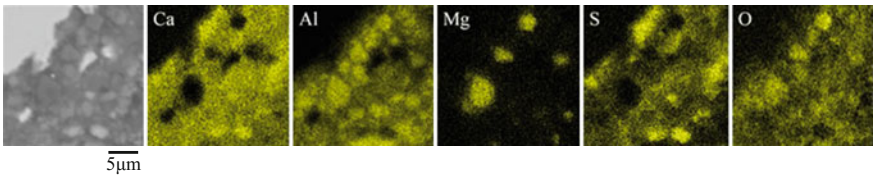

Fig. 6 Element mappings of a deposition on a ladle nozzle in the production of steel B

Conclusion

Plant experiments were carried out to study the formation and behavior of CaS inclusions in a steel melt during a secondary refining process without using a Ca-treatment. The inclusion characteristics in the steel samples taken at the end of an LF treatment and an RH treatment were determined using an SEM in combination with an EDS. Furthermore, thermodynamic calculations were performed to discuss the possibilities of forming CaS inclusions in steels without a Ca-treatment. Also, the influence of the interfacial properties between the inclusions and steel melts on the behavior of the observed inclusions in the steel melts was discussed. Based on the results of this study, the following conclusions can be drawn.

In a high-S steel melt, a CaS phase can be formed even when a Ca-treatment has not been used. Specifically, this can take place in two manners: a reaction between Ca and S, and a reaction between CaO in inclusions and S.

Due to the formation of a CaS phase, inclusions in high-S containing steel melts are covered by a CaS layer, which is difficult to remove from the melts. Therefore, the castability of high-S containing steels can be deteriorated by a deposition of CaS inclusions even without a Ca-treatment.

References

1. Holappa L (2001) Inclusion control for castability of resulphurized steels. In: Proceedings of the annual steelmaking conference, Warrendale, USA, pp 765–777
2. Cramb AW, Jimbo I (1989) Calculation of the interfacial properties of liquid steel—slag systems. Steel Res Int 60:157–165
3. Janke D, Ma Z, Valentin P, Heinen A (2000) Improvement of castability and quality of continuously cast steel. ISIJ Int 40:31–39
4. Fruehan RJ (1997) Future steelmaking technologies and the role of basic research. Metall Mater Trans A 28:1963–1973
5. Kawakami K, Taniguchi T, Nakashima K (2007) Generation mechanisms of non-metallic inclusions in high-cleanliness steel. Tetsu-to-Hagané 93:743–752
6. Yoshioka T, Nakahata K, Kawamura T, Ohba Y (2016) Factors to determine inclusion compositions in molten steel during the secondary refining process of case-hardening steel. ISIJ Int 56:1973–1981
7. Yoshioka T, Shimamura Y, Karasev A, Ohba Y, Jönsson P (2017) Mechanism of a CaS formation in an Al-killed high-S containing steel during a secondary refining process without a Ca-treatment. Steel Res Int 87, online published (srin. 201700147)
8. Yoshioka T, Ideguchi T, Karasev A, Ohba Y, Jönsson P (2017) The effect of a high Al content on the variation of the total oxygen content in the steel melt during a secondary refining process. Steel Res Int 87, online published (srin. 201700287)
9. Higuchi Y, Shirota Y, Obana T, Ikenaga H (1991) Behavior of inclusion in molten steel during RH treatment. CAMP-ISIJ 4:266
10. Mikhailov GG, Baibulenko EP (1981) Thermodynamics of interaction processes of oxygen and sulphur with calcium in liquid iron. Steel USSR 11:443–444
11. Verein Deutscher Eisenhuttenleute (1995) Slag Atlas, 2nd edn. Verlag Stahleisen GmbH Dusseldorf, Germany
12. Inoue R, Suito H (1994) Calcium desulfurization equilibrium in liquid iron. Steel Res Int 65:403–409
13. Hino M, Ito K (2010) Thermodynamic data for steelmaking. Tohoku University Press, Sendai
14. Cho SW, Suito H (1994) Assessment of calcium-oxygen equilibrium in liquid iron. ISIJ Int 34:265–269
15. Fujisawa T, Inoue S, Takagi S, Wanibe Y, Sakao H (1985) Solubility of CaS in the molten CaO-Al_2O_3-CaS slags and the equilibrium between the slags and molten steel. Tetsu-to-Hagané 71:839–845
16. Todoroki H, Mizuno K (2003) Variation of inclusion composition in 304 stainless steel deoxidized with aluminum. ISS Trans I&SM 30:60–67
17. Deng Z, Zhu M (2013) Evolution mechanism of non-metallic inclusions in Al-killed alloyed steel during secondary refining process. ISIJ Int 53:450–458
18. Yang W, Zhang L, Wang X, Ren Y, Liu X, Shan Q (2013) Characteristics of inclusions in low carbon Al-killed steel during ladle furnace refining and calcium treatment. ISIJ Int 53:1401
19. Arai H, Matsumoto K, Shimasaki S, Taniguchi S (2009) Model experiment on inclusion removal by bubble flotation accompanied by particle coagulation in turbulent flow. ISIJ Int 49:965–974
20. Zheng X, Hayes PC, Lee H-G (1997) Particle removal from liquid phase using fine gas bubbles. ISIJ Int 37:1091–1097
21. Cho J-S, Lee H-G (2001) Cold model study on inclusion removal from liquid steel using fine gas bubbles. ISIJ Int 41:151–157

22. Staronka A, Gotas W (1979) Investigations into the wettability of solid oxide and sulphide phases with pure iron melts and stainless steel melts. Arch Eisenhüttenw 50:237–242
23. Ogino K (1975) Interfacial tension between molten iron alloys and molten slags. Tetsu-to-Hagané 61:2118–2132
24. Poirier DR, Yin H, Suzuki M, Emi T (1998) Interfacial properties of dilute Fe-O-S melts on alumina substrates. ISIJ Int 38:229–238

Desulfurization of Copper-Iron Reduced from Copper Slag

Bao-jing Zhang, Ting-an Zhang, Li-ping Niu, Zhi-he Dou, Zhi-qiang Li and Dong-liang Zhang

Abstract In order to maximize the use of copper slag, a new idea that copper slag is reduced to smelt copper-containing antimicrobial stainless steel was proposed. But copper-iron reduced from copper slag contains a large number of copper matte, making sulfur content high. In this article, desulfurization of copper-iron was studied. The Fact-Sage software was used to calculate ΔG of the desulfurization reaction. Calcium oxide, calcium carbide and ferromanganese were used as desulfurization agent. The results show that desulfurization capacity of calcium oxide is poor, but with addition of carbon, desulfurization effect of calcium oxide will be enhanced. Calcium carbide and ferromanganese have good desulfurization effect.

Keywords Desulfurization · Copper-iron · Calcium oxide · Calcium carbide Ferromanganese

Introduction

With the development of copper smelting process, strong oxidation process is put into practice. Copper matte grade is higher, and copper element in smelting slag is also higher [1]. At present, the most common use of copper slag is that copper slag is diluted to obtain copper matte and tailings. Matte is back to copper smelting process, and tailings are made into cement, which make copper slag used with low value [2–7]. Based on this, our group proposed a new technology that copper slag is reduced to smelt copper containing antimicrobial stainless steel. That is, copper slag is directly reduced to obtain copper-containing molten iron, and then by a series of

B. Zhang · T. Zhang (✉) · L. Niu · Z. Dou · Z. Li · D. Zhang
Key Laboratory of Ecological Metallurgy of Multi-metal Intergrown Ores of Ministry of Education, Special Metallurgy and Process Engineering Institute, Northeastern University, Shenyang 110819, China
e-mail: zta2000@163.net

G. Lambotte et al. (eds.), *Materials Processing Fundamentals 2018*,
The Minerals, Metals & Materials Series,
https://doi.org/10.1007/978-3-319-72131-6_2